Eur. J. Inorg. Chem. **2014** · © WILEY-VCH Verlag GmbH & Co. KGaA, 69451 Weinheim, 2014 · ISSN 1099–0682

SUPPORTING INFORMATION

DOI: 10.1002/ejic.201301424
Title: Luminescent AgAu Alloy Clusters Derived from Ag Nanoparticles – Manifestations of Tunable Au^{I}–Cu^{I} Metallophilic Interactions
Author(s): Kumaranchira R. Krishnadas, Thumu Udayabhaskararao, Susobhan Choudhury, Nirmal Goswami, Samir Kumar Pal, Thalappil Pradeep*

Supporting Information 1

Procedure for polyacrylamide gel electrophoresis (PAGE):
A gel electrophoresis unit with 1 mm thick spacer (Bio-rad, Mini-protein Tetra cell) was used to process the PAGE. The total contents of the acrylamide monomers were 30% (bis(acrylamide:acrylamide) = 7:93) and 3% (bis(acrylamide:acrylamide) = 6:94) for the separation and condensation gels, respectively. The eluting buffer consisted of 192 mM glycine and 25 mM tris(hydroxymethylamine). The cluster was dissolved in 5% (v/v) glycerol-water solution (1.0 mL). The sample solution (1.0 mL) was loaded onto a 1 mm gel and eluted for 4 h at a constant voltage of 100 V to achieve separation.

Supporting Information 2

UV-vis spectra of the AgAu@MSA cluster and AgAuNPs formed during galvanic displacement reaction

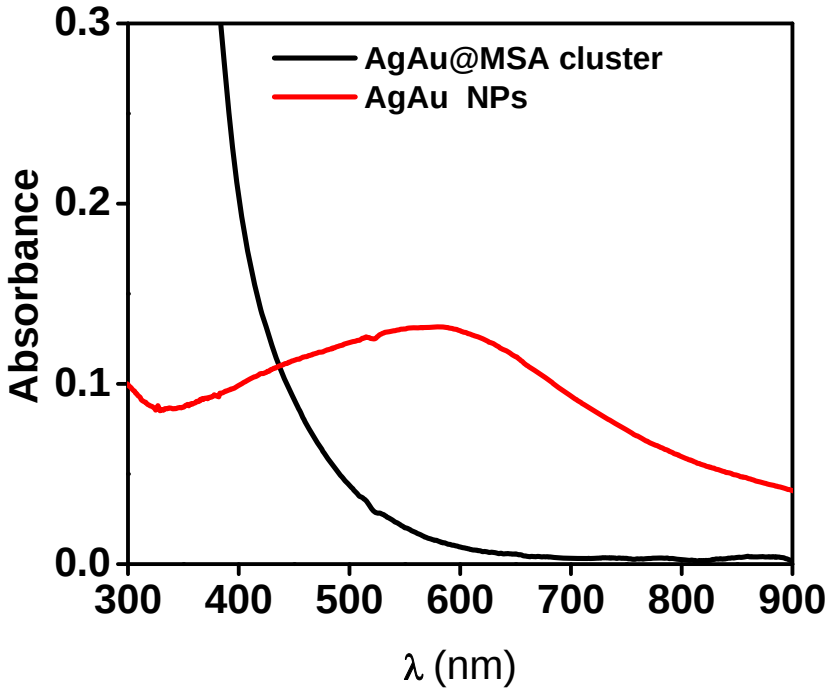

Figure S1. UV-vis spectra of the product (AgAu@MSA) and the byproduct (AgAuNPs) after the reaction between AgNPs and Au^{I}-MSA thiolate.

Supporting Infromation 3

XRD pattern of AgCl formed during galvanic displacement reaction

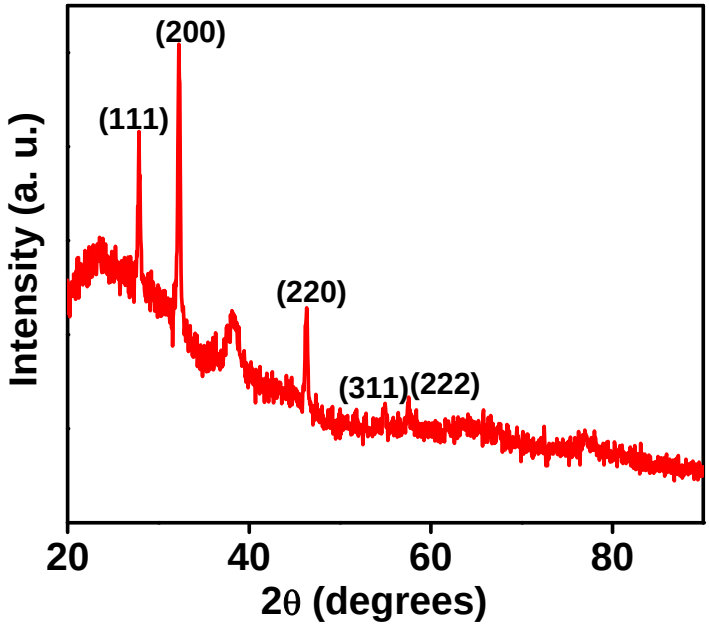

Figure S2. XRD pattern of the precipitate obtained after the reaction between AgNPs and the Au^{I}-MSA thiolate, in methanol. The peaks are due to the AgCl crystals formed during the galvanic displacement reaction. The peak at around 37 may be due to the AgAuNPs formed.

Supporting Information 4

Time-dependent evolution of luminescence during galvanic displacement reaction

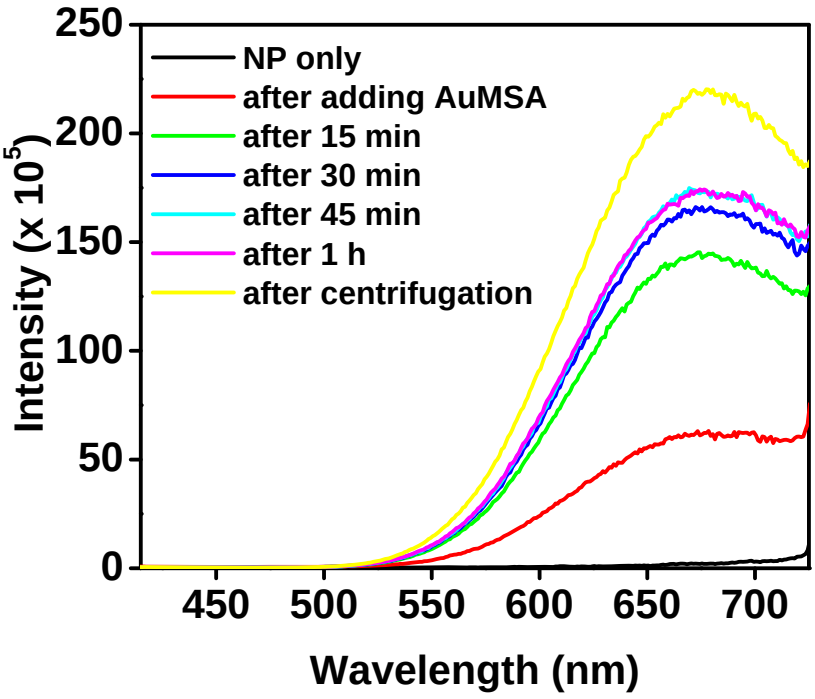

Figure S3. Time-dependent evolution in the photoluminescence showing the formation of AgAu@MSA clusters during the galvanic exchange reaction.

Supporting Information 5

EDAX spectrum and elemental composition of the AgAu@MSA cluster

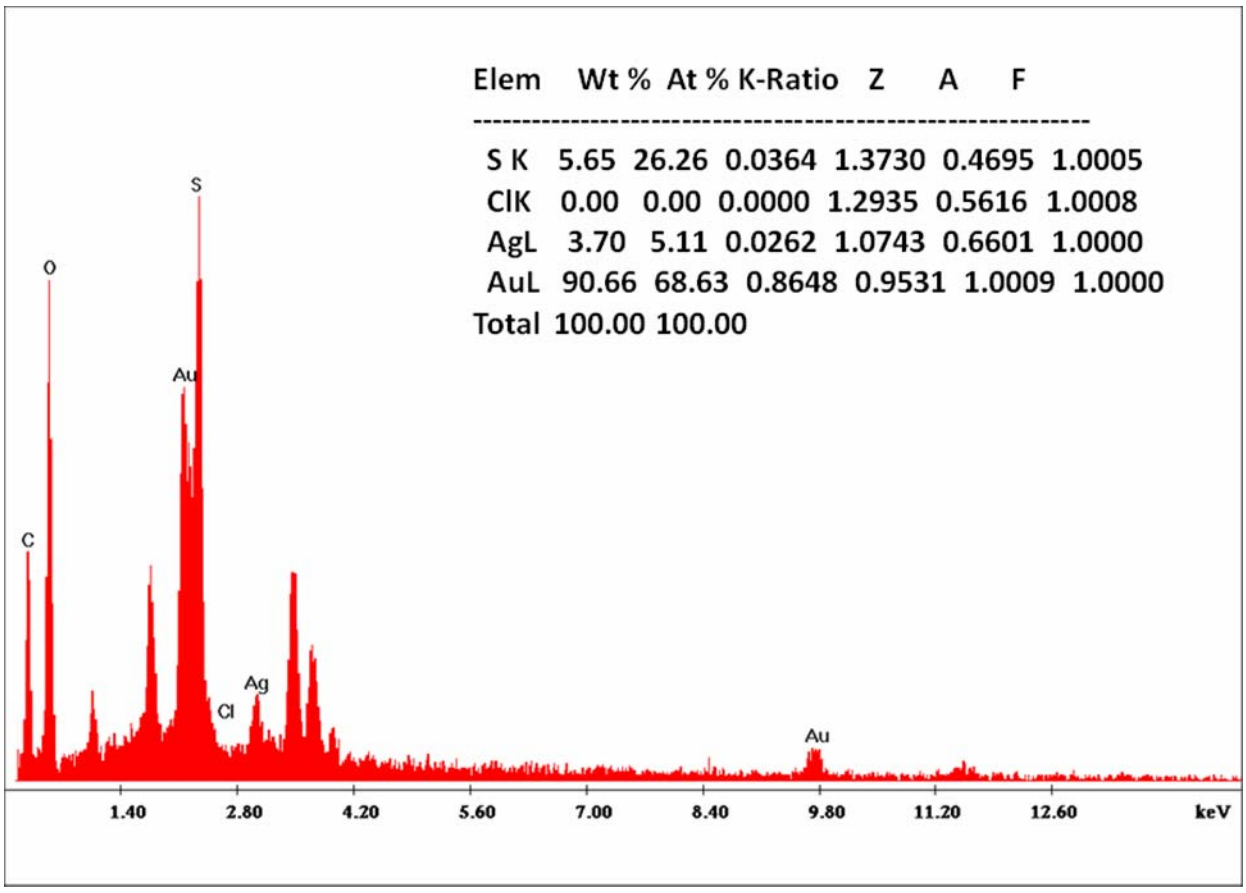

Figure S4. EDAX spectrum and elemental composition of the AgAu@MSA cluster.

Supporting Information 6

UV-vis spectra of the clusters in methanol with and without Cu^{II}

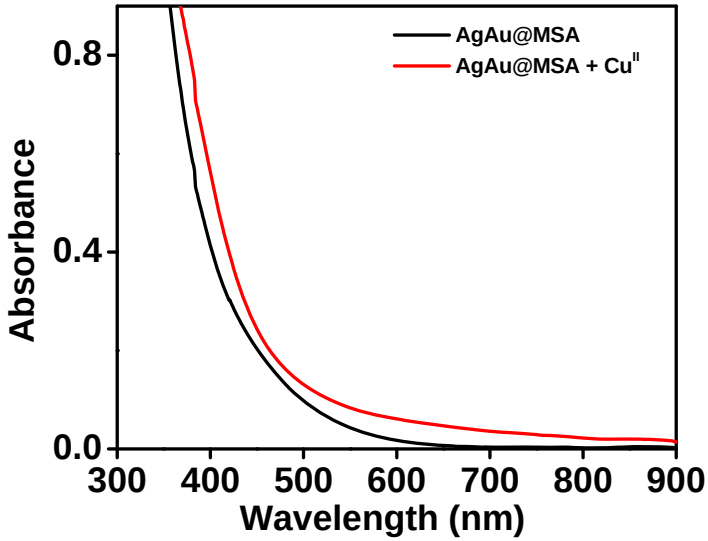

Figure S5. UV-vis absorption spectra of AgAu@MSA clusters in methanol with and without Cu^{II}.

Supporting Information 7

Photoluminescence data showing the ability of OA to prevent metal ion quenching

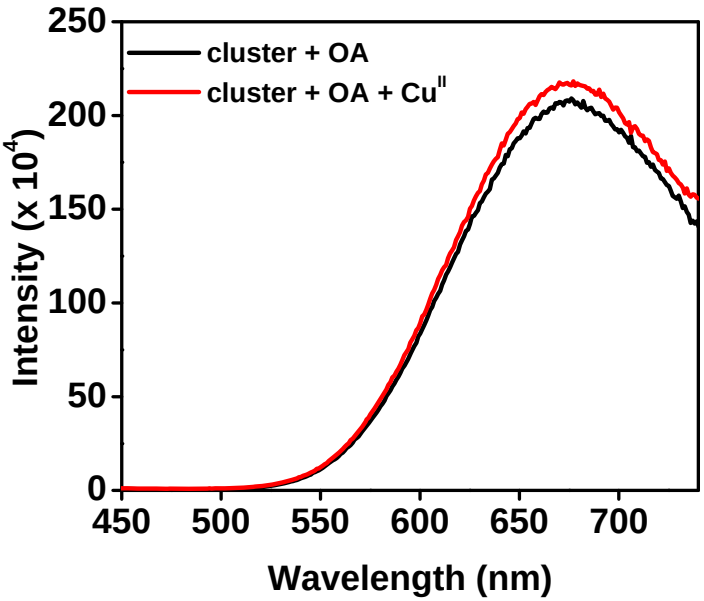

Figure S6. Emission spectra of the AgAu@MSA cluster solution in methanol containing oxalic acid and its stability of fluorescence upon the addition of Cu^{II}.

Supporting Information 8

Ag 3d regions in the XPS spectra of pure and Cu^{II}-treated clusters

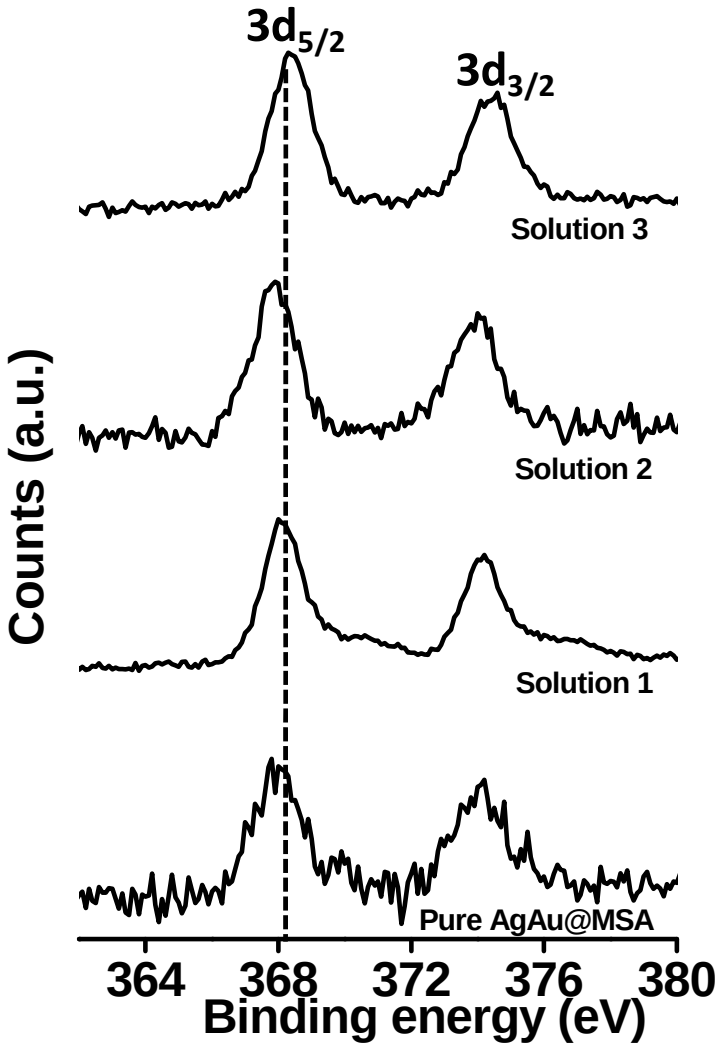

Figure S7. Ag 3d regions in the X-ray photoelectron spectra of pure and Cu^{II}-treated AgAu@MSA clusters.

Supporting Information 9

Lifetime measurements of alloy clusters containing different concentrations of Cu^{II}

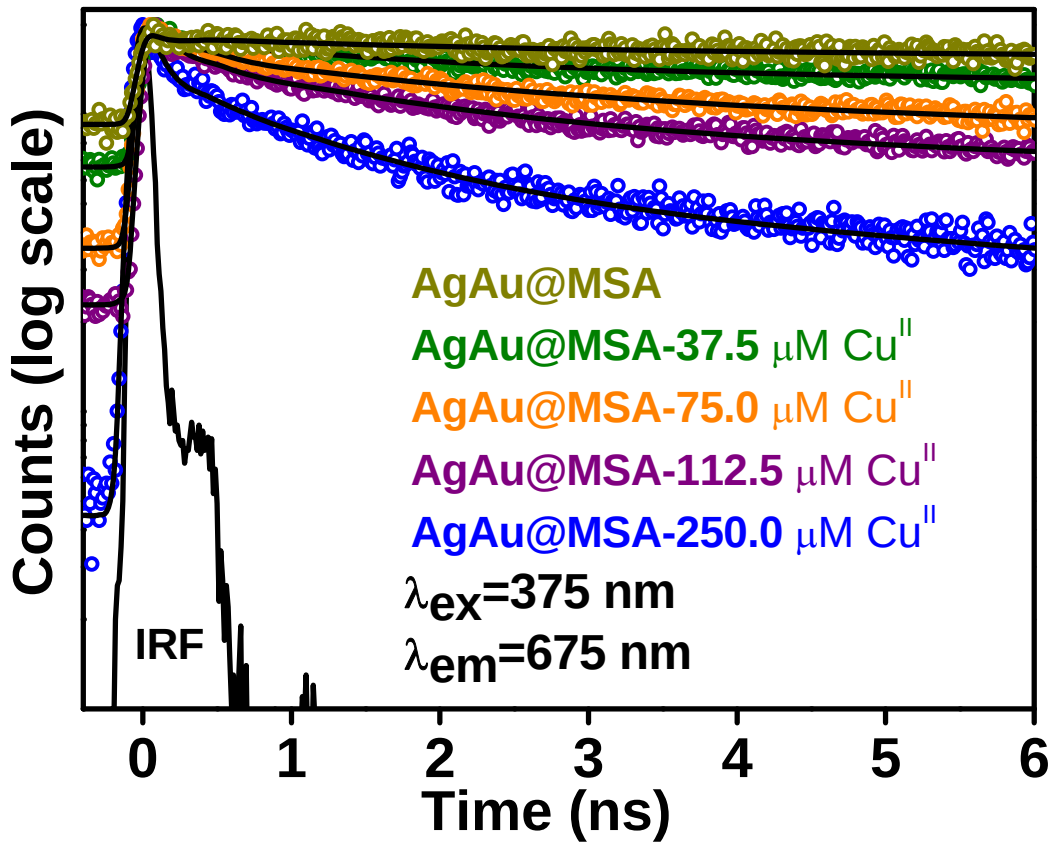

Figure S8. Picosecond time-resolved fluorescence transients of AgAu@MSA clusters containing different concentration of Cu^{II} in methanol.

Table S1. Picosecond time-resolved luminescence transients of AgAu@MSA clusters containing different concentration of Cu^{II} in methanol . The luminescence of these clusters (λ_{max} = 675 nm) is measured using a 375 nm excitation laser.

Concentration of Cu^{II} added to AgAu@MSA cluster in methanol	**τ_1 ns (%)**	**τ_2 ns (%)**	**τ_3 ns (%)**	**τ_{av} (ns)**
0	0.16 (38)	1.12 (20)	50.00(42)	21.28
37.5 μM	0.14 (42)	1.77 (21)	46.77 (37)	17.88
75 μM	0.12 (46)	1.75 (26)	30.45(28)	8.95
112.5μM	0.11(54)	1.60(26)	24.08(20)	5.36
250 μM	0.10 (65)	1.24 (22)	12.00 (13)	1.93

Supporting Information 10

Lifetime decay profiles and fitting parameters of solutions 2 and 3

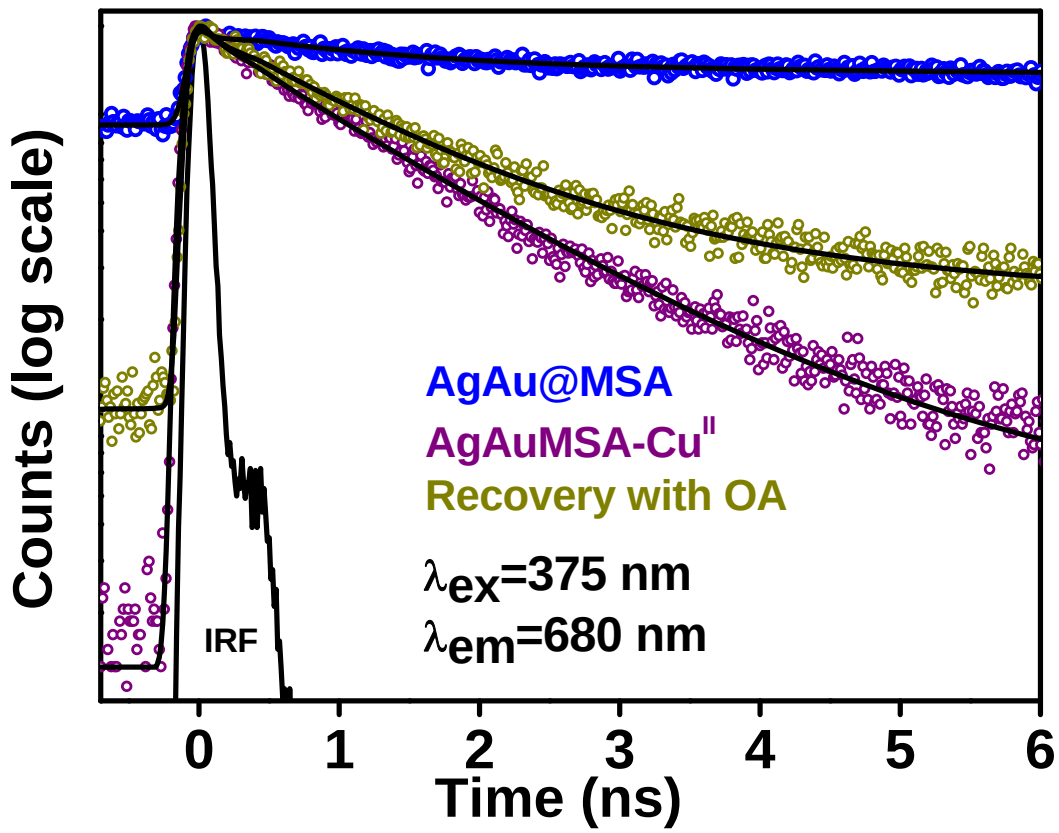

Figure S9. Picosecond time-resolved fluorescence transients of AgAu@MSA clusters in THF showing the quenching of the luminescence lifetime upon the addition of Cu^{II} and its partial recovery upon the addition of OA.

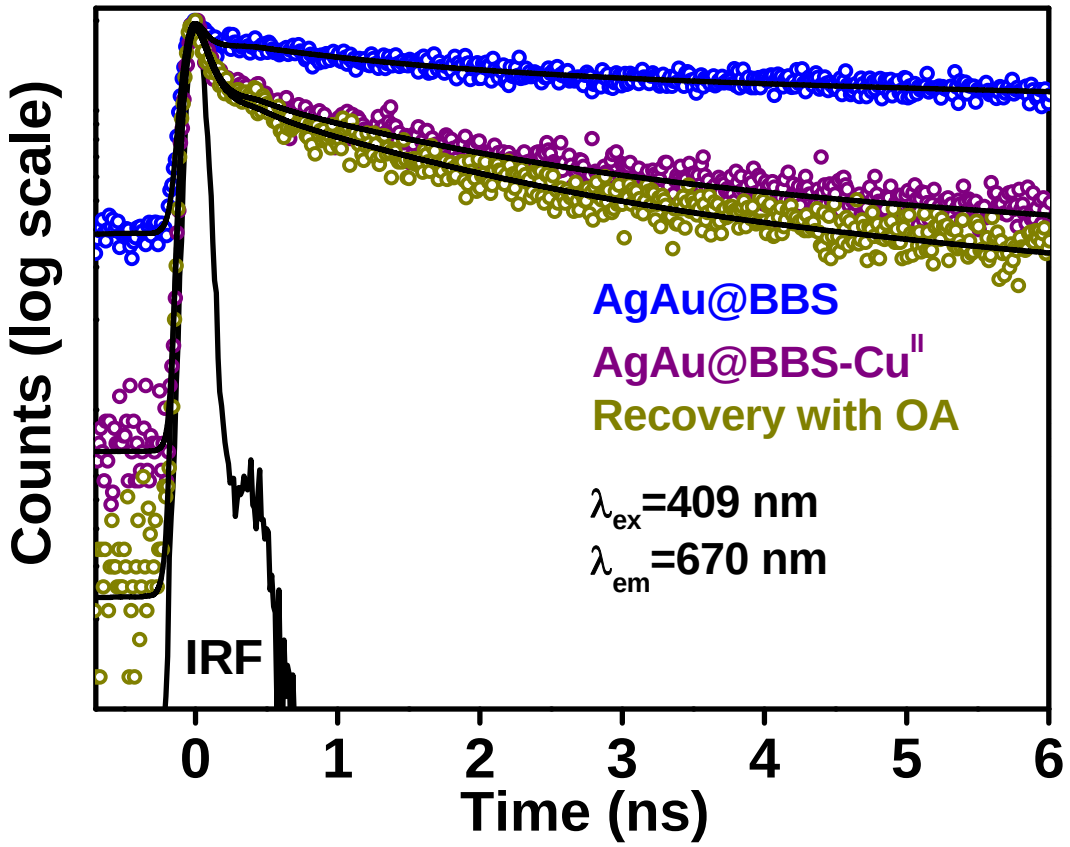

Figure S10. Picosecond time-resolved fluorescence transients of AgAu@BBS clusters in THF showing the quenching of the luminescence lifetime upon the addition of Cu^{II} and its irreversibility upon the addition of OA.

Table S2. Picosecond time-resolved luminescence transients of pure and Cu^{II}-treated AgAu@MSA cluster in THF. The luminescence of these clusters (λ_{max} = 680 nm) is measured using a 375 nm excitation laser.

Cluster system	τ_1 ns (%)	τ_2 ns (%)	$\tau_3$ns (%)	τ_{av} (ns)
Pure AgAu@MSA cluster in THF	0.24(23)	1.24 (35)	48.37 (42)	20.74
Cluster with Cu^{II}	0.18 (27)	1.44 (70)	15.56 (3)	1.39
Cluster with OA	0.21 (25)	1.45 (68)	32.28(7)	3.38

Table S3. Picosecond time-resolved luminescence transients of pure and Cu^{II}-treated AgAu@BBS cluster in THF. The luminescence of these clusters (λ_{max} = 670 nm) is measured using a 409 nm excitation laser.

Cluster system	$\tau_1$ns (%)	τ_2 ns (%)	$\tau_3$ns (%)	τ_{av} (ns)
AgAu@BBSH cluster in THF	0.15 (43)	2.5 (19)	41.12 (38)	21.28

Cluster with Cu^{II}	0.082 (71)	1.81 (17)	18.51 (12)	2.60
Cluster with OA	0.106 (69)	1.84 (19)	15.09 (12)	2.17

Supporting Information 11

Luminescence data showing the complete reversibility of the quenching in acetone as solvent

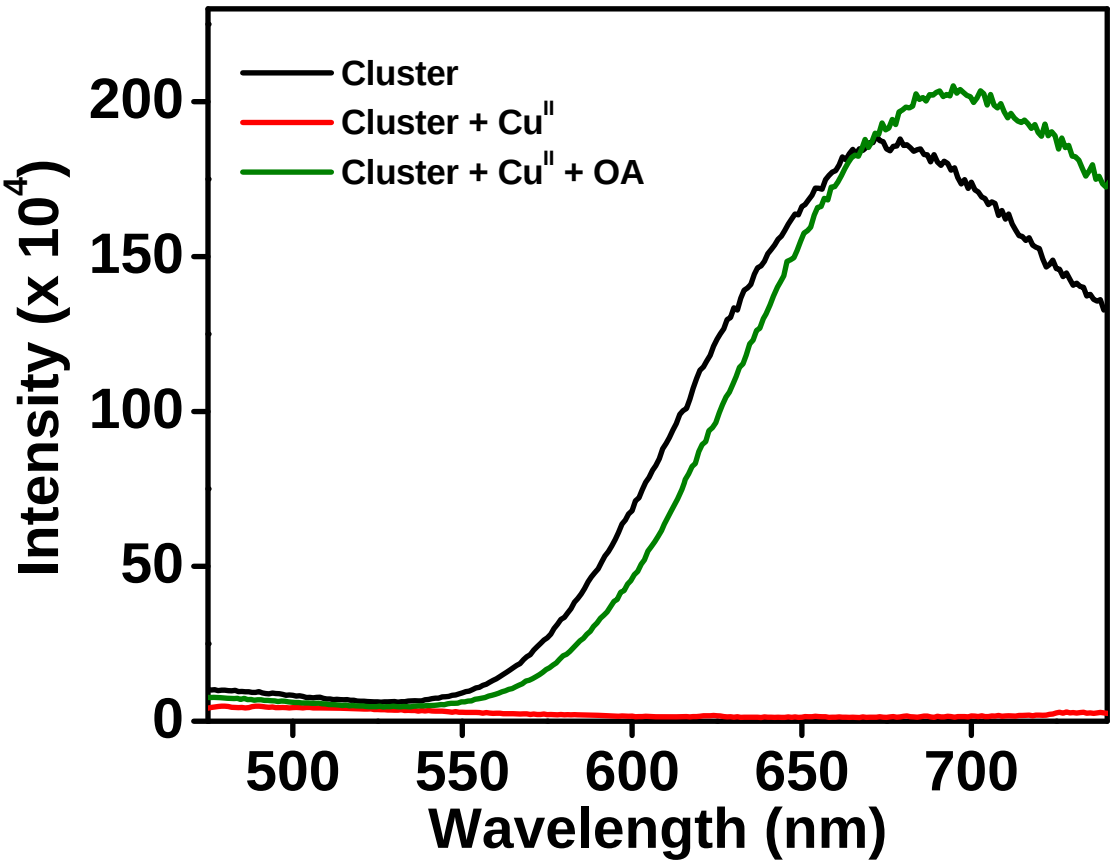

Figure S11. Luminescence data showing the quenching of the luminescence of AgAu@MSA clusters in acetone upon the addition of Cu^{II} and its complete recovery upon the addition of OA.